Light-Responsive Oligothiophenes Incorporating Photochromic Torsional Switches

ARTICLE

Light-Responsive Oligothiophenes Incorporating Photochromic Torsional Switches (PTS) Motif

Received 00th January 20xx,
Accepted 00th January 20xx

DOI: 10.1039/x0xx00000x

Augustina Jozeliūnaitė,[a,b] Aiman Rahmanudin,[d] Saulius Gražulis,[f] Emilie Baudat,[e] Kevin Sivula,[d] Daniele Fazzi,[c]* Edvinas Orentas,[b]* and Giuseppe Sforazzini [a]*[†]

We present a quaterthiophene and sexithiophene that can reversibly change their effective π-conjugation length *via* photoexcitation. The reported compounds make use of light-responsive molecular actuators consisting of an azobenzene attached to a bithiophene unit by both direct and linker-assisted bonding. Upon exposure to 350 nm light the azobenzene undergoes *trans*-to-*cis* isomerization mechanically inducing the oligothiophene to assume a planar conformations (extended π-conjugation). Exposure to 254 nm wavelenght promotes azobenzene *cis*-to-*trans* isomerization, forcing the thiophenic backbones to twist out of planarity (confined π-conjugation). Twisted conformations are also reached by *cis*-to-*trans* thermal relaxations with rate that increases proportionally with the conjugation length of the oligothiophene moiety. The molecular conformations of quaterthiophene and sexithiophene were characterized using steady-state UV-vis, X-ray crystallography and quantum-chemical modelling. Finally, we tested the proposed light-responsive oligothiophenes into field-effect transistors to probe the photo-induced tuning of their electronic properties.

Introduction

Conjugated compounds have been widely investigated as active component in numerous optoelectronic applications including light emitting diodes,[1-5] solar cells,[5-10] field effect transistors,[11-13] lasers,[14-17] and sensors.[18-22] Continuous efforts on the development of smart molecular design with thoughtful structure-property relationships, and control of the intermolecular interactions in the bulk, has allowed this class of molecules to reach unprecedented diffusion into commercial applications, e.g. OLED screens and automotive lighting. A common approach to tune the optical and electronic properties of conjugated compounds is by the functionalization of the π-system with electron-releasing or electron-withdrawing substituents.[23,24] At the same time, it is well-known that these properties strongly depend on the geometry of the π-system. Thus, varying the regioregularity or tuning the steric interactions of lateral substituents are also the most common strategies used to tailor the physical properties of conjugated systems.[24-29] The strong optical response induced by twisting the π-system has been successfully applied, for instance, in thiophene derivatives for ion[19-20] and viscosity sensing.[30-32] The use of chemical trigger to tune the effective conjugation length of π-systems, however, is not compatible with the environmental insulation of optoelectronic devices that is necessary for their correct functioning and good lifetime.[33] Thus, molecular designs that exploit non-chemical stimuli, such as light, are the best candidate to create responsive organic semiconductors for the development of new optoelectronic technologies.[34,35] To date, examples of light-responsive molecular actuators conceived to tune the effective conjugation length of linear π-systems have been mainly based on two paradigms: the cleavage-formation of π-bonds,[36-39] and the torsion-planarization of p-orbitals nodal plane.[40-42] The first class of compounds, e.g. diarylethenes, is generally incorporated as monomeric unit into π-conjugated backbone of oligomers and polymers, the second, instead, is usually placed as a side-functionality along linear π-conjugated systems. Recently Peters et al. have shown that diarylethenes can be also engineered as a side-functionality to tune the planarization of the π-system.[43] Despite the inherent differences in the molecular design of two aforementioned categories of compounds, their functionality suffers from some limitations.

[a.] *Laboratory of Macromolecular and Organic Materials, Institute of Material Science and Engineering, Ecole Polytechnique Federale de Lausanne (EPFL), 1015 Lausanne, Switzerland.*
[b.] *Department of Organic Chemistry, Faculty of Chemistry and Geosciences, Naugarduko 24, LT-0325, Vilnius, Lithuania.*
[c.] *Università di Bologna, Dipartimento di Chimica "Giacomo Ciamician", Via F. Selmi, 2, 40126 Bologna, Italy.*
[d.] *Laboratory for Molecular Engineering of Optoelectronic Nanomaterials, École Polytechnique Fédérale de Lausanne (EPFL), 1015 Lausanne, Switzerland.*
[e.] *Institute of Biotechnology, Vilnius University, Saulėtekio al. 7, LT-10257 Vilnius, Lithuania.*
[f.] *Institute of Chemical Sciences and Engineering, Ecole Polytechnique Federale de Lausanne (EPFL), 1015 Lausanne, Switzerland.*

† Present address: Department of Chemical and Geological Sciences, Università degli Studi di Cagliari, SS 554, bivio per Sestu, 09042 Monserrato, Cagliari, Italy.

‡ Electronic Supplementary Information (ESI) available: Synthetic procedures, NMR spectra, conformational sampling (CREST and GFN2-xTB methods), DFT and TDDFT calculations, excited states assignments, X-ray structures. *See DOI: 10.1039/x0xx00000x*

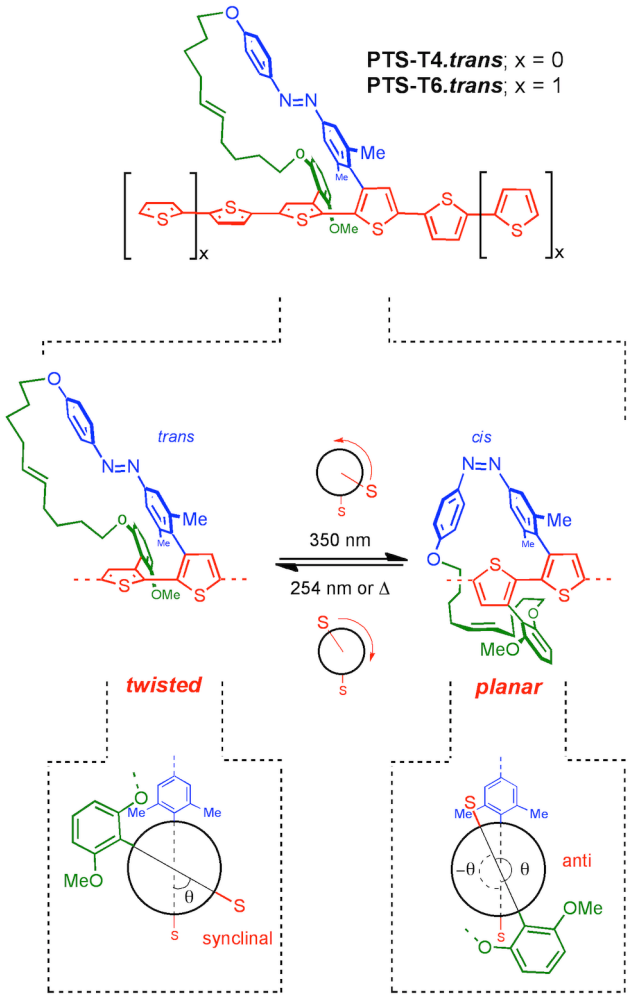

Figure 1. Schematics of molecules studied in this work.

Molecular architectures that rely on the cleavage-formation of π-bonds often reduce their operation reversibility efficiency as their π-conjugation extension increases.[44-47] On the other hand, the design of the molecular actuators that modulate the π-bond geometry of a conjugated system are commonly restricted to the possibility to assume only semiplanar conformations (e.g. *syn* and *anti*) that are similar in their electronic structures.[40-42]

In the present work, we changed the usual design and molecular architecture of light-responsive π-conjugated compounds. We introduced a light-driven molecular switch (azobenzene) in an orthogonal fashion to a linear π-conjugated system (oligothiophene), thus to suppress the detrimental reduction of switchability due to the π-conjugation extension. At the same time, a side-chain linker, connecting the azobenzene to bithiophene unit allows for the achievement of highly twisted π-bond geometry in the linked bithiophenic segment. The described macrocyclic architecture (molecular actuactor) consisting of an azobenzene, a linker and a bithiophene is referred to as photochromic torsional switch (PTS) unit.[48] In order to modulate the effective conjugation length of a linear π-system, the PTS unit was positioned at the centre of the presented compounds. Herein we report on the quaterthiophene and the sexithiophene comprising the PTS unit that can reversibly tune the π-conjugated extension along their backbones using light as an external stimulus. The proposed PTS-based architectures can be of potential interest as active component in novel light-responsive optoelectronic devices.

Result and Discussion

Synthesis and Molecular XRD Molecular Characterization

The synthesis of the PTS-based oligothiophenes was achieved as summarized in Figure 2a. First the PTS unit (**PTS-T2**) was prepared through a convergent route affording the sole *trans-twisted* conformer.[26] The latter was then functionalized in both 2-positions of thiophene rings using LDA followed by I_2 or thimethylthin chloride, to achieve the corresponding 2,2'-halides (**1**) and 2,2'-stannanes (**2**) derivatives. The PTS-based quaterthiophene (**PTS-T4.*trans***) and hexathiopnene (**PTS-T6.*trans***) were synthesized by Suzuki and Stille coupling of PTS bithiophene 2,2'-halides and 2,2'-stannanes, respectively, with mono-functionlized thiophene and bithiophene bearing complement functionalities (for details about the synthesis, see ESI). Single crystals of **PTS-T2**, **PTS-T4**, and **PTS-T6** molecules were grown from tetrahydrofuran solution using vapor diffusion of hexane. The X-ray crystallographic analysis of **PTS-T2**, **PTS-T4**, and **PTS-T6** revealed atropo-enantiomers packed in centrosymmetric P21/c, P-1 and C2/c unit cells, respectively (for more details on the cell unit and packing see ESI). The dihedral angles (θ) between the two PTS thiophenic subunits were found to be θ = 60° for the pristine PTS unit **PTS-T2**, θ = 57° and θ = 58° for **PTS-T4**, and **PTS-T6**, respectively (Figure 2b). The oligothiophene backbone assumes a twisted geometry at the center, decoupling the two halves (subunits) that are planar.

Analysis of the packing shows that in the case of **PTS-T2**, which lacks lateral aromatic extension, no close contacts between thiophene rings were observed. In **PTS-T4**, the terminal thiophene rings of two neighbouring molecules adopts slipped π-π staking arrangement, also exhibiting S…S interaction ($d_{S\text{-}S}$ = 3.6 Å, Figure 2c), often observed in solid state structures of sulfur containing compounds.[49] The stacked dimer is further surrounded from both sides by nearly orthogonal thiophene rings. The **PTS-T6** displayed similar packing pattern featuring π-π stacked dimer surrounded by thiophene rings (Figure 2d). In contrast to **PTS-T4**, the thiophene rich regions in **PTS-T6** involve stacking and orthogonal T arrangement (edge-to-face) between extended dithiophene regions rather than single thiophene rings as in **PTS-T4**, suggesting its possibly better charge conducting properties.[50] Moreover, stacking of thiophene rings in **PTS-T6** is realized in parallel fashion with respect to sulfur atoms whereas in **PTS**-T4 antiparallel arrangement is observed (for details see ESI).

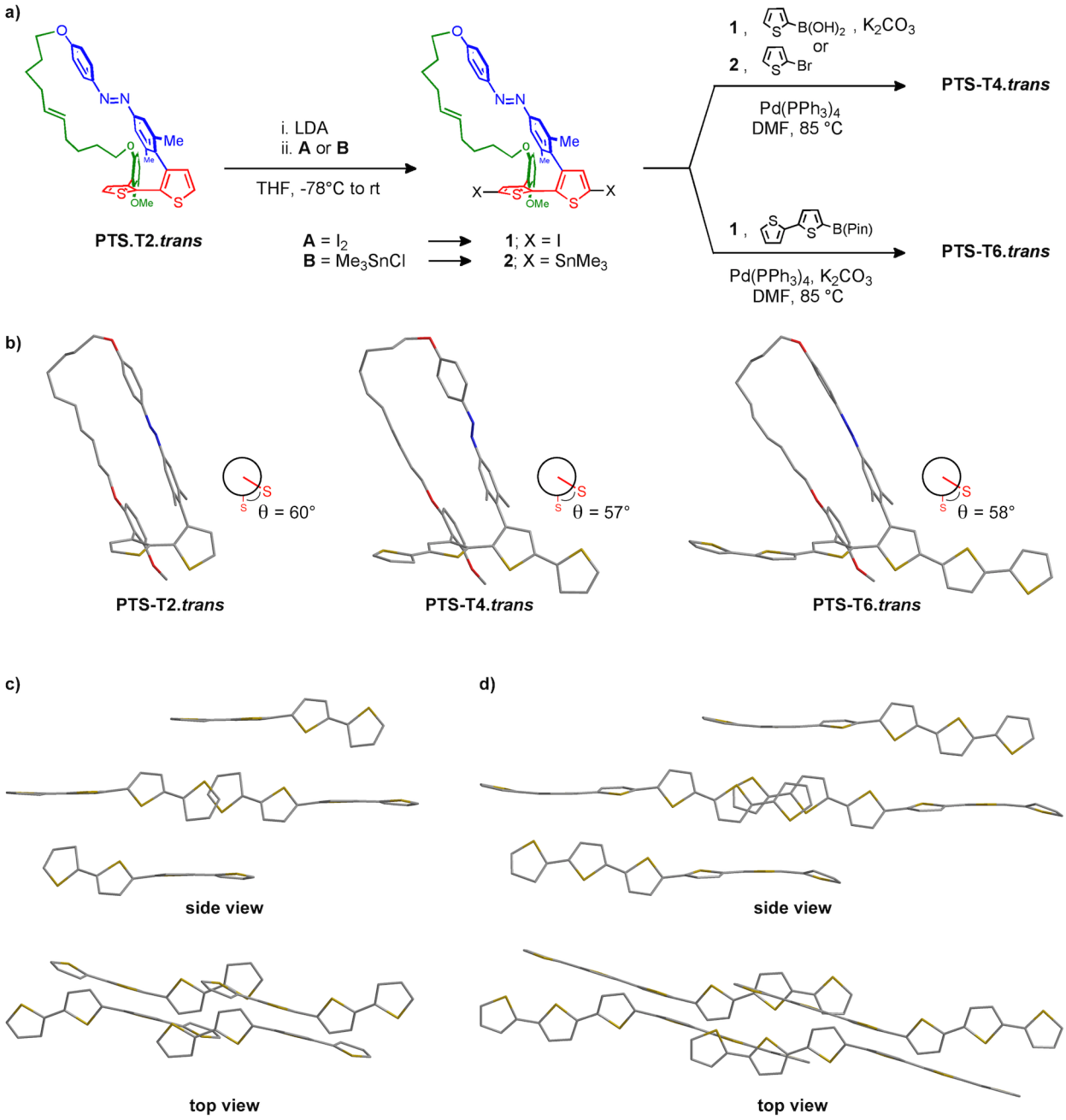

Figure 2. (a) Synthetic pathway for **PTS-T4** and **PTS-T6** from the PTS unit **PTS-T2**. (b) X-ray single-crystal structure of **PTS-T2.*trans***, **PTS-T4.*trans*** and **PTS-T6.*trans***. (c) Selected parts of the solid state structures **PTS-T4.*trans*** showing arrangement of thiophene units. (d) Selected parts of the solid state structures **PTS-T6.*trans*** showing arrangement of thiophene unit.

Spectroscopic Characterization and Quantum Chemical Modeling

The absorption spectra of the *trans* PTS derivatives, **PTS-T4.*trans*** and **PTS-T6.*trans***, exhibit absorption spectra with a main broad band at 358 nm and 379 nm, respectively (Figure 3a). The signatures of these two spectra differ significantly from that of the pristine **PTS-T2.*trans*** where the contributions of the two constituting components, the bithiophene and the azobenzene, are well distinguishable with a band at 284 nm for the former and a peak centred around 363 nm for the latter.[48] The observed broad band in the absorption spectrum of **PTS-T4.*trans*** and **PTS-T6.*trans*** can be attributed to a spectral overlap of the electronic transition of the azobenzene and that of the oligothiophene backbone. As the azobenzene is disposed orthogonally to the thiophenic π-systems, it is not expected to undergo any significant change in its absorption spectrum with the elongation of the thiophene-based chain.

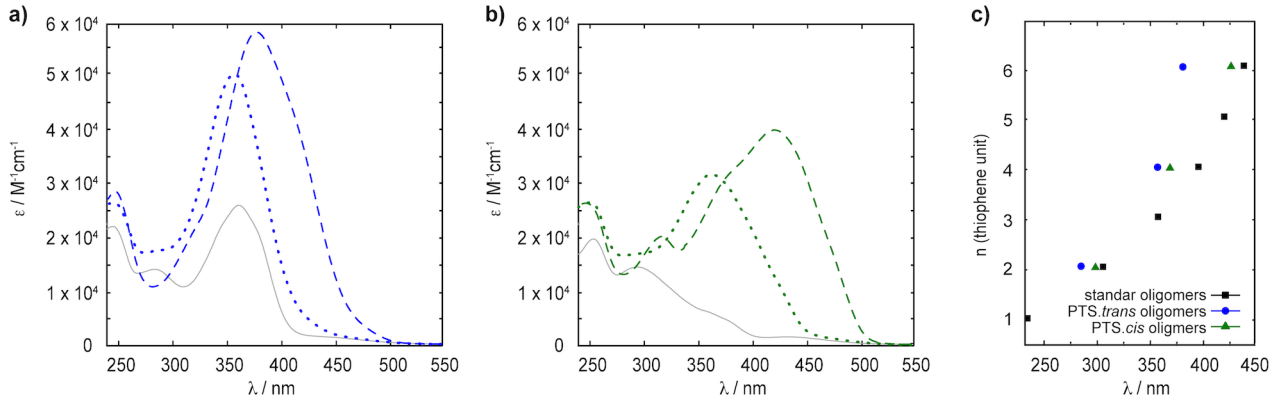

Figure 3. (a) Absorption spectra of **PTS-T2.*trans*** (grey solid line), **PTS-T4.*trans*** (blue dotted line), and **PTS-T6.*trans*** (blue dashed line) in THF diluted solutions. (b) Absorption spectra of **PTS-T2.*cis*** (grey solid line), **PTS-T4.*cis*** (green dotted line), and **PTS-T6.*cis*** (green dashed line) in THF diluted solutions. (c) Plot with the absorption λ_{max} of **PTS-T2**, **PTS-T4**, and **PTS-T6** in their twisted-trans (blue) and planar-cis (green) forms, and selected pristine oligothiophenes (di-, tert-,quater-, penta-, sexi- thiophenes, black) reported in literature [51]

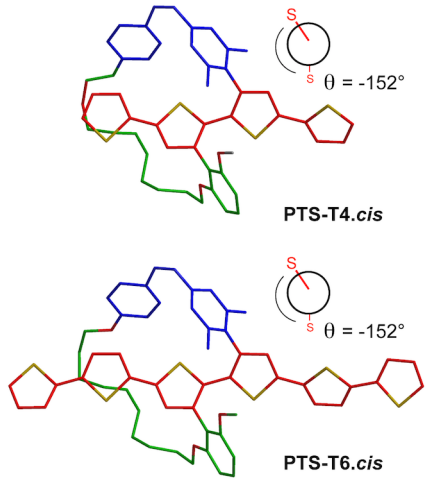

Figure 4. DFT (ωB97X-D/6-311+G*) optimized geometries of **PTS-T4.*cis*** and **PTS-T6.*cis*** by TDDFT calculations.

However, the gradual π-extension from the bithiophene to the sexithiophene lowers the excitation energy of the thiophenic backbone resulting in a spectral shift towards longer wavelengths. The anticipated bathochromic shift might cause a superimposition with the absorption band of the azobenzene (λ_{max} = ~363 nm). Considering that the PTS motif twists the oligothiophene backbone in its middle, we could expect that the spectral contribution of the twisted quaterthiophene in **PTS-T4.*trans*** is red-shifted with respect to that of its half segment (bithiophene, λ_{max} = ~303 nm) and blue-shifted with respect to its extended form (quaterthiophene, λ_{max} = ~392 nm), Figure 3c.[51] Similarly, the twisted backbone of **PTS-T6.*trans*** can be expected to have its absorption band between that of the terthiophene (λ_{max} = ~354 nm) and that of an extended sexiathiophene (λ_{max} = ~436 nm), Figure 3c.[51] To get insights into the excited states of **PTS-Tn.*trans*** and better characterize the band overlap in the UV-Vis spectra, we performed excited state quantum-chemical calculations on lowest-energy conformers, as obtained by a combined tight-binding DFT-based approach and further full DFT refinements (see ESI and computational methods).[52-54] According to time dependent density functional theory (TDDFT),[55] the observed absorption band of both **PTS-T4.*trans*** (358 nm) and **PTS-T6.*trans*** (379 nm) involves two competing electronic transitions: one, here called $S_0 \rightarrow S^*_{thio}$, that is localized on the oligothiophene chain, and another one, named $S_0 \rightarrow S^*_{azo}$, that is localized on the azobenzene unit. For **PTS-T4.*trans*** the $S_0 \rightarrow S^*_{thio}$ is ascribed to the $S_0 \rightarrow S_3$ one-electron transition that is mainly described as the highest occupied molecular orbital (HOMO) to the lowest unoccupied molecular orbital (LUMO)+1 transition, both orbitals localized on the thiophenic backbone. The $S_0 \rightarrow S^*_{azo}$ is associated to the $S_0 \rightarrow S_2$ transition prevalently involving the HOMO-1 to LUMO, the latter mainly localized on the azobenzene (see ESI, Section 5). TDDFT calculations show that the two transitions are 13 nm apart one from the other, so confirming the superimposition between the absorption bands of the quaterthiophene and the azobenzene. In the case of **PTS-T6.*trans***, the $S_0 \rightarrow S^*_{thio}$ is characterized by the $S_0 \rightarrow S_2$ one-electron transition prevalently described as HOMO → LUMO+1 of the backbone, while the $S_0 \rightarrow S^*_{azo}$ involves multiple one-electron transitions with the HOMO-1 → LUMO as dominant. These two competing transitions lie in close proximity within 17 nm, so confirming a spectral overlap between the absorption bands of sexithiophene and that of azobenzene (see ESI, Section 5). In addition, TDDFT calculations show that by extending the thiophenic chain, from **PTS-T4.*trans*** to **PTS-T6.*trans***, the $S_0 \rightarrow S^*_{thio}$ transition undergoes a bathochromic shift of ~30 nm, in accordance to the increased ***π***-electron conjugation of the oligothiophene unit (see ESI, Section 5.2). Upon irradiation at 350 nm approximately 49% of **PTS-T4.*trans*** and 57% of **PTS-T6.*trans*** are converted to their *cis-planar* isomers. The absorption spectrum of the former exhibits one main broad band centred at ~366 nm (Figure 3b), which is blue-shifted of about 26 nm with respect to the λ_{max} of a regular quaterthiophene, (Figure 3c).[51]

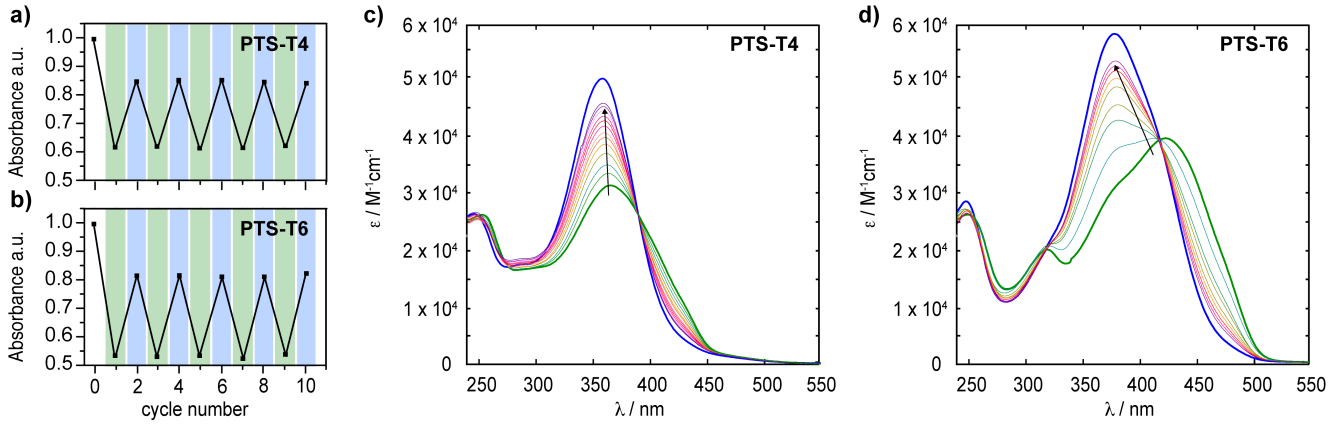

Figura 5. (a) Photoswitching of **PTS-T4**. (b) Photoswitching of **PTS-T6**. (c) Thermal relaxation from-*cis*-to-*trans* of **PTS-T4** in THF diluted solutions at 25°C. (g) Thermal relaxation from-*cis*-to-*trans* of **PTS-T6** in THF diluted solutions at 25°C.

The observed hypsochromic shift can be ascribed to the parasite spectral contributions involving the twisted-quaterthiophene and the azobenzene, in its *trans* and *cis* forms. Such a scenario is plausible as **PTS-T4** reaches a photostationary state (PSS) once is irradiated at 350 nm. In the case of **PTS-T6.*cis*** the absorption spectrum shows three distinguishable bands: a main one at 424 nm, a shoulder at 387 nm, and one at 319 nm (Figure 3b). The first and the third bands are significantly close to the wavelengths commonly reported for a pristine sexithiophene (λ_{max} = 436 nm and λ = 314 nm).[51] This finding suggests that the planar arrangement assumed by the oligothiophene backbone upon photo-isomerization of the azobenzene to its cis form is reasonably close to the structure of the pristine sexithiophene. However, the band at 387 nm indicates the presence of competitive absorbing species that generate a PSS for **PTS-T6**.

In order to understand the correlation between the absorption spectra and the structural changes induced by the azobenzene to the oligothiophene backbone, we first computed the **PTS-T4.*cis*** and **PTS-T6.*cis*** lowest-energy conformers, by performing as for the case of **PTS-Tn.*trans*** a multi-level conformational screening followed by TDDFT calculations. It has to be noted, that the computational investigations were essential to determine the equilibrium molecular structures of **PTS-T4.*cis*** and **PTS-T6.*cis***, as these compound spontaneously return to their initial *trans-twisted* conformation within the day, so hampering the possibility to grow crystals. DFT calculations of **PTS-T4.*cis*** and **PTS-T6.*cis*** show that when the azobenzene is in its *cis* form the oligothiophene backbone assumes a more planar conformation with θ = 152.4˚ and 152.3˚, respectively (Figure 4). The latter values are in good agreement within the range of dihedral angles reported in literature for unsubstituted bi-, quater-, sexi- thiophenes in their *anti*-conformation (θ = 146°-152°).[56,57] According to TDDFT calculations, performed for the most stable conformers, the main bands in the computed absorption spectra of **PTS-T4.*cis*** and **PTS-T6.*cis*** can be assigned to the sole $S_0 \rightarrow S^*_{thio}$ transition, deriving from the $S_0 \rightarrow S_2$ excitation mainly involving HOMO and LUMO which are prevalently localized on oligothiophene chain (anti conformation, see ESI, Section 5). By the analysis of DFT and TDDFT calculations, we can deduce that when the azobenzene isomerizes from-*trans*-to-*cis* it reduces the dihedral angle of the central bithiophene and at the same time assists the planarization of the whole oligothiophenic backbone. The adoption of these planar conformations results in a remarkable optical response from the oligothiophene moiety, with a bathochromic shift for the $S_0 \rightarrow S^*_{thio}$ transition of 42 nm for **PTS-T4** and of 37 nm for **PTS-T6**. As anticipated, the main absorption bands measured for **PTS-T4.*cis*** and **PTS-T6.*cis*** still have significant contributions from the electronic transitions of the unconverted **PTS-T4.*trans*** and **PTS-T6.*trans*** (both $S_0 \rightarrow S^*_{thio}$ and $S_0 \rightarrow S^*_{azo}$). Thus, while for **PTS-T6** the spectral shift from the *trans-twisted* to the *cis–planar* forms is well visible, for **PTS-T4** is less pronounced.

Photoswitchability and Thermal Relaxation

PTS-based oligothiophene **PTS-T4** and **PTS-T6** can reversibly switch between their *trans-twisted* and *cis-planar* forms. After their *trans*-to-*cis* isomerization **PTS-T4** and **PTS-T6** can recover about ~83% and ~79% of the initial absorption intensity by irradiating at 254 nm (Figure 5a-b).[58] The wavelength was selected as an alternative excitation to the usual n - π^* transition for the *cis*-to-*trans* isomerization which, in the alkoxyazobenzenes, is usually ascribed to an absorption band around ~440 nm.[59,60] The latter is inaccessible in our systems due to the competitive absorption of the oligothiophenic backbone. Moreover, the structural constrain of azobenzene in the PTS-derivatives leads to a similar oscillator strengths for the n - π^* transition of the *trans* and *cis* conformers, so making excitation at this absorption band is moderately effective for *cis*-to-*trans* isomerization. Excitation around 250 nm promote the ϕ - ϕ^* transition of azobenzenes which exhibits not influence from the structural constraint of the PTS architecture.[60]

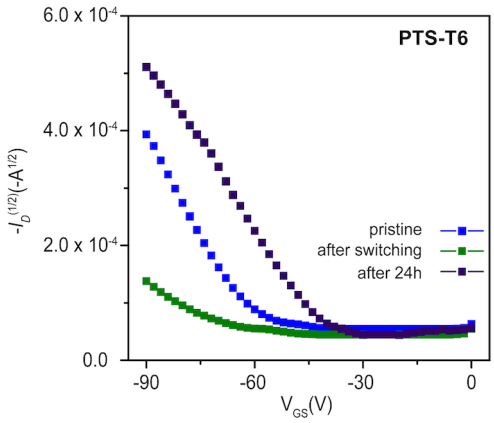

Figure 6. Transfer curves of **PTS-T6** in bottom gate bottom contact field effect transistor.

In contrast to what we previously published for the *cis* form of the parent PTS unit (**PTS-T2**) in its *cis* form, **PTS-T4*.cis*** and **PTS-T6*.cis*** return spontaneously to their trans forms by thermal relaxation within 1-1.5 days. In addition, the velocity of this process increases directly with the extension of the thiophene-based backbone π-conjugation. **PTS-T4** and **PTS-T6** recover about ~95% of the initial absorption intensity within 36h and 24h respectively (Figure 5c-d). These enhanced thermal relaxations are unexpected as the structural constraint of the PTS unit is retained in both **PTS-T4** and **PTS-T6**, and as the extension at of π-conjugation take place along the oliothiophenes backbone and not on the azobenzene. The analysis of the computed frontier molecular orbitals of PTS derivatives shows that the lengthening of the thiophenic backbone π-conjugation (from T4 to T6) increases the overlap and the cross-conjugation between the localized molecular orbitals of the azobenzene unit and those of the thiophenic chain (see ESI, Figure S4). The electronic coupling between these pseudo-orthogonal frontier orbitals induces a polarization along the azobenzene unit with an electron-rich area onto the phenolic segment, and a relatively electron-poor part around dimethylbenzene. This effect is particularly evident for the **PTS-T6*.trans*** species, characterized by a strong electronic coupling between the localized orbitals of the azobenzene units and those of the sexithiophene chain, leading to a hybridized orbital picture (see ESI Figure S4). Such a scenario reassemble the electronic configuration of push-pull azobeneze that are known to have extremely short *cis* isomer life-time.[61] Thus, by extending the backbone π-conjugation of PTS-based architectures it is possible to tune the switching properties of the azobenzene moiety. To the best of our knowledge, the enhancement of the azobenzene *cis*-to-*trans* thermal relaxation with the increasing conjugation of an orthogonally attached π-system has never reported before.

Electron Mobility

To investigate if the conformational changes induced by the azobenzene to the conjugated backbone affects the charge transport properties of the PTS derivatives, we fabricated bottom gate bottom contact transistors containing PTS-based oligothiophens as the active semiconducting layer (for details see ESI, Section 6). Thin-films of **PTS-T4** and **PTS-T6** were solution processed via spin coating in its *trans-twisted* form and its hole mobility (μ_h) was measured. Transistors containing **PTS-T4*.trans*** did not exhibit any charge transport, while **PTS-T6*.trans*** displayed a μ_h of 4 x10^{-6} cm^{-2}/Vs, Figure 6. The latter was then irradiated with UV light at a wavelength of 350 nm for (10 min) and its transistor performance measured. After irradiation, the charge mobility decreased to μ = 5 x10^{-7} cm^{-2}/Vs, but recovered to μ = ~ 3.5 x10^{-5} cm^{-2}/Vs after storing in the dark for 24 hrs under nitrogen in a glovebox (see ESI, Section 6). The observed reduction of charge transport can be ascribed to the change in molecular packing induced by the photo-activated *trans*-to-*cis* isomerization of the PTS unit as discussed above. Meanwhile the recovery of the charge transport is likely due to the azobenzene undergoing a *cis*-to-*trans* isomerization over time. However, the enhanced charge mobility upon recovering the initial *trans-twisted* conformation might suggest that PTS-based molecules have assumed a more efficient packing for charge percolation after a full cycle compared to the as prepared film. This promising preliminary result governs a further in-depth investigation that is currently on-going and will be reported elsewhere.

Conclusions

A novel class of light-responsive oligothiophenes was synthetized using the PTS architecture as molecular-actuator. PTS-based quaterthiophene and sexithiophene reversibly tune their optical properties in response to light, and exhibit an enhanced thermal relaxation proportional to their backbone π-conjugation extension. Moreover, a preliminary investigation on their use as active layer in OFETs suggests that the proposed PTS-based derivatives can be successfully used for the development of a new generation of light-responsive optoelectronic devices.

Conflicts of interest

The authors declare no conflicts to declare

Acknowledgements

G.S would like to thank Prof. Holger Frauenrath for his helpful discussions, and the Swiss National Science Foundation (SNSF) Ambizione program (PZ00P2_148050) for the financial support.

Notes and references

1 A. Salehi, X. Fu, D. Shin, F. So, *Adv. Funct. Mater.* 2019, **29**, 1808803.
2 L. Cao, Z. Zhu, K. Klimes, J. Li, *Adv. Mater.* 2021, **33**, 2101423.
3 J. Bauri, R. B. Choudhary, G. Mandal, *J. Mater. Sci.*, 2021, **56**, 18837–18866.

4 M. J. Frampton, *et al. Adv. Funct. Mater.*, 2008, **18**, 3367–3376.
5 S. Brovelli , G. Sforazzini, M. Serri , G. Winroth , K. Suzuki, F. Meinardi , H. L. Anderson, F. Cacialli, Adv. Funct. Mater. 2012, **22**, 4284–4291.
6 C. Lee, S. Lee, G. Kim, W. Lee, B. J. Kim, *Chem. Rev*. 2019, **119**, 8028−8086.
7 S. Shoaee, A. L. Sanna and G. Sforazzini, *Molecules*, 2021, **26**, 7439.
8 A. Rahmanudin, R. Marcial-Hernandez, A. Zamhuri, A. S. Walton, D. J. Tate, R. U. Khan, S. Aphichatpanichakul, A. B. Foster, S. Broll and M. L. Turner, *Advanced Science*, 2020, 2002010.
9 R. Zhou1, Z. Jiang, C. Yang, J. Yu, J. Feng, M. A. Adil, *Nat. Commun.,* 2019, **10**, 5393.
10 Y. Cui, *et al. Adv. Mater.*, 2021, **33**, 2102420.
11 Q. Meng, W. Hu, *Phys. Chem. Chem. Phys.,* 2012, **14**, 14152–14164.
12 K. Liu, B. Ouyang, X. Guo, Y. Guo and Y. Liu, *npj Flexible Electronics*, 2022, 1–19.
13 Y. Yu, Q. Ma, H. Ling, W. Li, R. Ju, L. Bian, N. Shi, Y. Qian, M. Yi, L. Xie, W. Huang, *Adv. Funct. Mater.*, 2019, **29**, 1904602
14 T. Schmaltz, G. Sforazzini, T. Reichert and H. Frauenrath, *Adv. Mater.*, 2017, **29**, 1605286.
15 A. J. C. Kuehne and M. C. Gather, *Chem. Rev.*, 2016, **116**, 1–42.
16 Y. Jiang, Y.-Y. Liu, X. Liu, H. Lin, K. Gao, W.-Y. Lai and W. Huang, *Chem. Soc. Rev.*, 2020, **49**, 5885–5944.
17 M. M. Mróz, G. Sforazzini, Y. Zhong , K. S. Wong, H. L. Anderson, G. Lanzani, J. Cabanillas-Gonzalez, *Adv. Mater.*, 2013, **25**, 4347–4351.
18 H. Dong, H. Zhu, Q. Meng, X. Gong and W. Hu, *Chem. Soc. Rev.*, 2012, **41**, 1754–1808.
19 M. J. Marsella, T. M. Swager, *J. Am. Chem. Soc.*, 1993, **115**, 12214-12215.
20 A. Giovannitti, C. B. Nielsen, J. Rivnay, M. Kirkus, D. J. Harkin, A. J.P. White, H. Sirringhaus , G. G. Malliaras , I. McCulloch, *Adv. Funct. Mater.*, 2016, **26**, 514–523.
21 K. Sugiyasu, T. M. Swager, *Bull. Chem. Soc. Jpn*., 2007, **80**, 2074–2083.
22 Z. Ma, P. Chen, W. Cheng, K. Yan, L. Pan, Y. Shi, G. Yu, *Nano Lett.*, 2018, **18**, 4570−4575.
23 X. Guo, M. Baumgarten and K. Müllen, *Prog. Polym. Sci.*, 2013, **38**, 1832–1908.
24 J. Roncalli, *Macromol. Rapid Commun.,* 2007, **28**, 1761–1775.
25 H. S. O. Chan and S. C. NG, *Prog. Polym. Sci.*, 1998, **23**, 1167–1231.
26 D. Vonlanthen, A. Rudnev, A. Mishchenko, A. Käslin, J. Rotzler, M. Neuburger, T. Wandlowski and M. Mayor, *Chem. Eur. J.*, 2011, **17**, 7236–7250.
27 D. A. Doval, M. D. Molin, S. Ward, A. Fin, N. Sakai and S. Matile, *Chem. Sci.*, 2014, **5**, 2819–2825.
28 A. Bedi, A. M. Armon, Y. Diskin-Posner, B. Bogosalvsky, O. Gidron, *Nat. Commun.*, 2022, **13**, 451
29 C. Schaack, A. M. Evans, F. Ng, M. L. Steigerwald, C. Nuckolls, *J. Am. Chem. Soc.,* 2022, **144**, 42−51
30 A. Fin, A. V. Jentzsch, N. Sakai and S. Matile, *Angew. Chem. Int. Ed*., 2012, **51**, 12736–12739.
31 M. D. Molin, Quentin Verolet, A. Colom, R. Letrun, E. Derivery, M. Gonzalez-Gaitan, Eric Vauthey, A. Roux, N. Sakai and S. Matile, *J. Am. Chem. Soc*., 2015, **137**, 568−571.
32 M. D. Molin and S. Matile, *Org. Biomol. Chem.*, 2013, **11**, 1952–1957.
33 W. Su., Printed Electronics: Materials, Technologies and Applications, 1st Edition, 2016, Cap. 8
34 L. Yu, *et al.* J. Mater. Chem. C, 2022, **10**, 8874–8880
35 C. Liu, H. Lin, S. Li, H. Xie, J. Zhang, D. Ji, Y. Yan, X. Liu, W. Lai, *Adv. Funct. Mater.,* 2022, **32**, 2111276.
36 C. P. Harvey and J. D. Tovar, *Polymer Chemistry*, 2011, **2**, 2699–2706.
37 Francesco Stellacci, Chiaro Bertarelli, Francesca Toscano, Maria C. Gallazzi, Gianni Zotti, Giuseppe Zerbi, Adv. Mater. 1999, 11, 292-295.
38 T. Kawai, Y. Nakashima, M. Irie, Adv. Mater., 2005,17, 309-314.
39 H. Cho, E. Kim, Macromolecules, 2002, 35, 8684-8687
40 B. Jousselme, P. Blanchard, N. Gallego-Planas, J. Delaunay, M. Allain, P. Richomme, E. Levillain and J. Roncali, *J. Am. Chem. Soc.*, 2016, **125**, 2888–2889.
41 B. Jousselme, P. Blanchard, M. Allain, E. Levillain, M. Dias and J. Roncali, *J. Phys. Chem.*, 2066, **110**, 3488–3494.
42 V. A. Azov, J. Cordes, D. Schlüter, T. Dülcks, M. Böckmann and N. L. Doltsinis, *Journal of Organic Chemistry*, 2014, **79**, 11714−11721.
43 G. M. Peters, J. D. Tovar , *J. Am. Chem. Soc.*, 2019, **141**, 3146−3152.
44 A. Peters, N. R. Branda, *Adv. Mater. Opt. Electron.*, 2000, **10**, 245-249.
45 T. Kaieda, S. Kobatake, H. Miyasaka, M. Murakami, N. Iwai, Y. Nagata, A. Itaya, M. Irie, J. Am. Chem. Soc., 2002, **124**, 2015-2024.
46 T. Kawai, T. Sasaki, M. Irie, *Chem. Commun.*, 2001, 711–712
47 N. Tanifuji, M. Irie, K. Matsuda, *Chem. Lett.*, 2005, **34**, 1580-1581
48 J. Maciejewski, A. Sobczuk, A. Claveau, A. Nicolai, R. Petraglia, L. Cervini, E. Baudat, P. Miéville, D. Fazzi, C. Corminboeuf and G. Sforazzini, *Chem. Sci.*, 2017, **8**, 361.
49 L. Antolini, E. Tedesco, G. Barbarella, L. Favaretto, G. Sotgiu, M. Zambianchi, D. Casarini,| G. Gigli, R. Cingolani, *J. Am. Chem. Soc.*, 2000, **122**, 9006-9013.
50 Z. Yao, J. Wang, J. Pei, *Cryst. Growth Des.*, 2018, **18**, 7−15.
51 R. S. Becker, J. S. de Melo, A. N. L. Mac anita and F. Elisei, *J. Phys. Chem.*, 1996, **100**, 18683–18695.
52 C. Bannwarth, E. Caldeweyher, S. Ehlert, A. Hansen, P. Pracht, J. Seibert, S. Spicher, S. Grimme, *WIREs Comput. Mol. Sci.*, 2021, **11**, e1493.
53 S. Grimme, C. Bannwarth, P. Shushkov, *J. Chem. Theory Comput.*, 2017, **13**, 1989−2009.
54 C. Bannwarth, S. Ehlert, S. Grimme, *J. Chem. Theory Comput.*, 2019, **15**, 1652−1671
55 Note: TDDFT calculations were executed on fully optimized, lowest-energy DFT (ωB97X-D/6-311+G*) PTS trans conformers. The latters were initially obtained via a preliminary conformational screening based on the tight-binding DFT-based method GFN2-xTB (Geometry Frequency Non-covalent interactions-eXtended Tight Binding) coupled with meta-dynamics simulations via CREST (Conformer–Rotamer Ensemble Sampling Tool) algorithm, see details in ESI.
56 V. Hernandez and J. T. L. Navarrete, *J. Chem. Phys.*, 1994, **101**, 1369–1377.
57 T.-J. Lin and S.-T. Lin, *Phys. Chem. Chem. Phys.*, 2015, **17**, 4127–4136.
58 Note: For PTS-T4, ~83% of absorption intensity at 358 nm correspond to ~74% of PTS-T4.trans; for PTS-T6, ~79% of absorption intensity at 379 nm correspond to ~71% of PTS-T6.trans. Irradiation at 254 nm does not result in any isomerization of olefn double from *trans*-to-*cis* bond (see ESI).
59 N. Tamai and H. Miyasaka, *Chem. Rev.*, 2000, **100**, 1875−1890.
60 H. H, Jaffé, S. Yeh, R. W. Gardner, *J. Mol. Spectrosc.,* 1958, **2**, 129-136.
61 H. M. D. Bandara, S. C. Burdette, *Chem. Soc. Rev.*, 2012, **41**, 1809–1825.